IEEE Photonics Journal
An IEEE Photonics Society Publication

Polarization-Independent Two-Layer Grating With Five-Port Splitting Output Under Normal Incidence

Volume 12, Number 2, April 2020

Bowen Gong
Huiying Wen
Hongtao Li

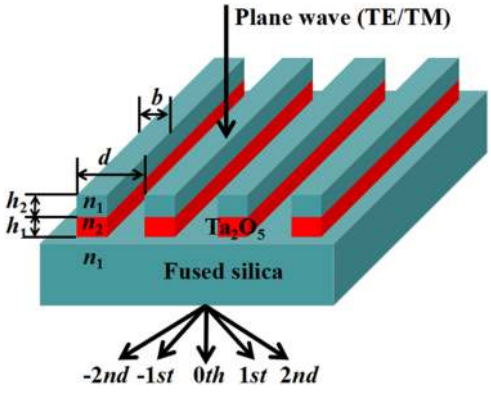

DOI: 10.1109/JPHOT.2020.2978882

Polarization-Independent Two-Layer Grating With Five-Port Splitting Output Under Normal Incidence

Bowen Gong,[1] Huiying Wen,[1] and Hongtao Li [2]

[1]Department of Engineering and Transportation, South China University of Technology, Guangzhou 510640, China
[2]Guangdong Provincial Key Laboratory of Optical Fiber Sensing and Communications, Institute of Photonics Technology, Jinan University, Guangzhou 511443, China

DOI:10.1109/JPHOT.2020.2978882

Manuscript received January 16, 2020; revised February 13, 2020; accepted March 3, 2020. Date of publication March 9, 2020; date of current version March 16, 2020. This work was supported by the National Natural Science Foundation of China under Grant 51578247. Corresponding authors: Huiying Wenand; Hongtao Li (e-mail: hywen@scut.edu.cn; 18814116735@163.com).

Abstract: In this paper, we report a two-layer five-port diffraction grating by a polarization-independent design under normal incidence. To be different from conventional five-port gratings, initially, we design a novel two-layer grating with operation in transmission. Next, we firstly design a polarization-independent grating with five-port splitting output. On the one hand, the accurate grating vector parameters are optimized using rigorous coupled-wave analysis (RCWA) approach. On the other hand, the inherent coupling mechanism happened in the grating region can be well explained by employing simplified modal method (SMM). More importantly, all reported conventional five-port beam splitter gratings were designed based on polarization dependent. Although they could obtain high diffraction efficiency for TE or TM polarization, it requires more complicated and time-consuming fabrication processes in practical grating applications. Thus, this work can open up a possible thought for designing polarization-independent multi-port beam splitter diffraction gratings.

Index Terms: Polarization independent, two-layer grating, five-port splitting output, RCWA, SMM.

1. Introduction

Polarization-Independent diffraction gratings are key optical diffraction elements, which can be found in potential optical applications in semiconductor optical amplifiers [1], polarization-independent filter [2], three-dimensional photonic integration [3], on-chip optoelectronic integration [4], two spectral beam combined fiber amplifiers [5] and so on. In most reported traditional works, design of numerous polarization-independent beam splitter gratings are excessively relied on numbers of different output diffraction orders. Generally, under Bragg incidence, it is very easy to design polarization-independent grating splitters (i.e., high-efficiency gratings [6]–[8], two-port gratings [9]–[11], polarization-selective gratings [12]–[14], polarizing beam splitter gratings [15]–[19]), because of the numbers of different output diffraction orders are no more than two for transverse-electric (TE) polarization or transverse-magnetic (TM) polarization. Under second Bragg incidence, It is relatively easy to obtain optimized polarization-independent high-efficiency grating [20] or two-port beam splitter grating [21]. Under normal incidence, three-port [22] and two-port [23],

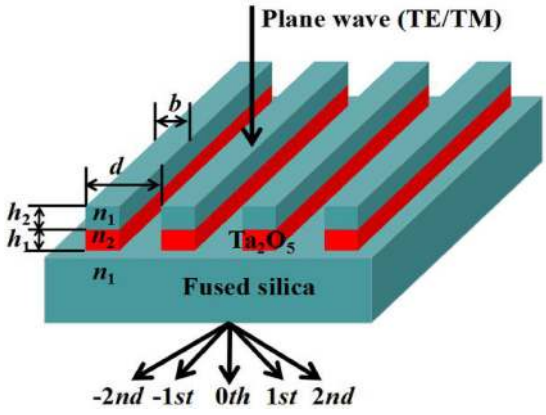

Fig. 1. The schematic diagram of our proposed two-layer polarization-independent five-port beam splitter transmission grating under normal incidence.

[24] zeroth-order cancelled polarization-independent diffraction gratings are also easily optimized by using RCWA [25] method and SMM [26].

Particularly, under second Bragg incident condition, because of efficiencies of three different output diffraction orders are difficulty to be optimized simultaneously for both TE and TM polarizations. Hence, polarization-dependent three-port beam splitter grating [27] was proposed, where the output different diffraction orders were the $-$2nd order, the $-$1st order and the 0th order, respectively. Similarly, under normal incident condition, some of five-port reflective or transmission beam splitter gratings [28], [29] are numerically optimized based on polarization-dependent designs, which are limited for applying in optical domains.

Herein, we firstly propose and numerically optimize a polarization-independent two-layer transmission five-port diffraction grating under normal incidence. Compared with reported reflective or transmission five-port beam splitter gratings, our proposed novel two-layer five-port grating element has merits of polarization-independent property and fine splitting performance for TE and TM polarizations simultaneously. Therefore, our designed five-port grating element can be found potential applications in optical measurement technology and three-dimensional holography.

2. Grating Design and Numerical Optimization

The schematic diagram of our designed grating is exhibited in Fig. 1. As exhibited in Fig. 1, such a polarization-independent grating basically consists of two-layer different grating ridges and a grating substrate. The materials of two-layer grating groove are fused silica and Ta_2O_5. Refractive indices of fused silica (n_1) and Ta_2O_5 (n_2) are 1.45 and 2.0, respectively. This grating structural parameters include grating depths (h_1 and h_2), grating period (d), grating duty cycle (the ratio of b to d). The TE-polarized wave or TM-polarized wave perpendicularly illuminates on polarization-independent two-layer grating. The incident wavelength is λ of 800 nm. The incident polarized wave can be coupled to diffraction orders. Based on our designed grating structure, the output diffraction orders are the $\pm$2nd orders, the $\pm$1 st orders and the 0th order, in which the $-$2nd order and the 2nd order or the $-$1st order and the 1st order are symmetric diffraction order. For simplifying our optimization process, we only consider efficiencies of the 1st order and the 2nd order in our numerical calculations.

In this design, we use numerical RCWA algorithm to optimize our proposed grating. RCWA algorithm can not only calculate the single-layer grating, but also it can optimize multi-layer grating parameters accurately. In this transmission grating structure, according to a series of fourier expansions, we can obtain the final diffraction efficiency for each diffraction order under the grating substrate. The obtained grating diffraction efficiency can be shown as follow for TE

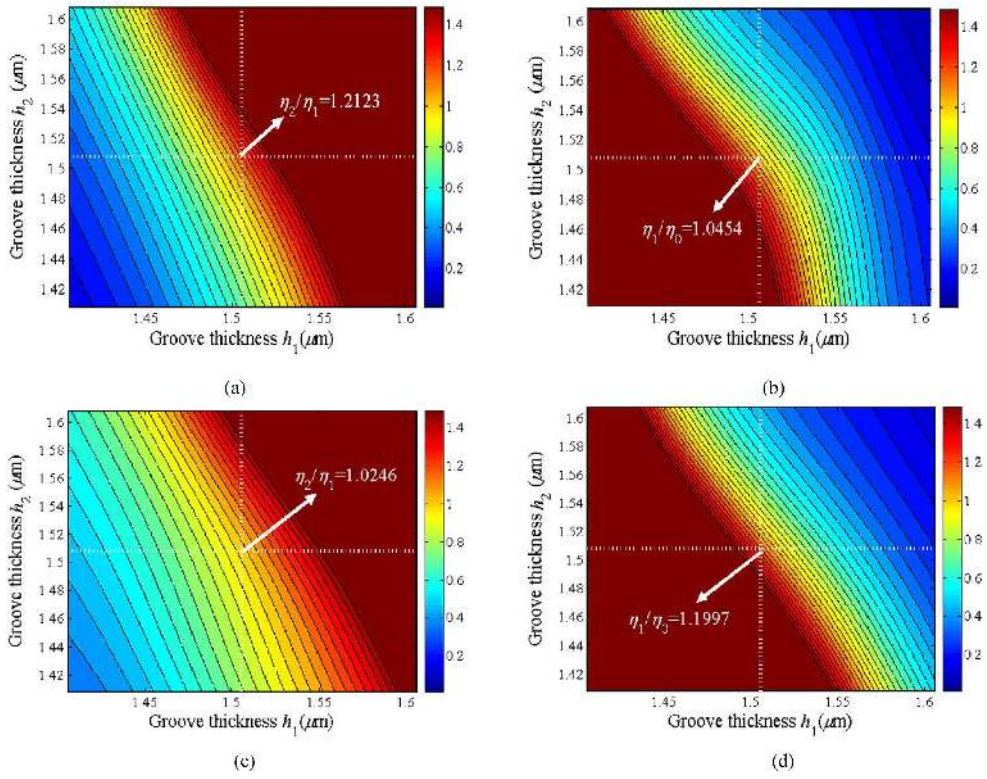

Fig. 2. Diffraction efficiency's ratios corresponding to the two-layer grating thicknesses with the optimized grating period of 3000 nm and duty cycle of 0.5 under normal incidence. (a) The ratio between the 2nd order and the 1st order for TE polarization. (b) The ratio between the 1st order and the 0th order for TE polarization. (c) The ratio between the 2nd order and the 1st order for TM polarization. (d) The ratio between the 1st order and the 0th order for TM polarization.

polarization [25]:

$$\eta_{ti}^{TE} = T_i T_i^* \mathrm{Re}\left(\frac{k_{zi}}{k_0}\right), \tag{1}$$

For TM polarization

$$\eta_{ti}^{TM} = T_i T_i^* \mathrm{Re}\left(\frac{k_{zi}}{k_0 n_1^2}\right), \tag{2}$$

Where

$$k_{zi} = \begin{cases} k_0\sqrt{n_1^2 - k_{xi}^2/k_0^2}, & k_0 n_1 > k_{xi} \\ -jk_0\sqrt{k_{xi}/k_0 - n_1^2}, & k_{xi} > k_0 n_1 \end{cases}, \tag{3}$$

Where

$$k_{xi} = -i\frac{2\pi}{d}, \tag{4}$$

$$k_0 = \frac{2\pi}{\lambda}, \tag{5}$$

T_i indicates the normalized electric-field or magnetic-field amplitude of the ith diffracted wave.

Fig. 2 shows the optimized diffraction efficiencies versus the grating groove thicknesses of h_1 and h_2. As can be seen from Fig. 2, with the optimized grating period of 3000 nm, the incident

TE-polarized wave and TM-polarized wave can be splitted into five diffraction order with equal energy. The efficiency's ratios of the 2nd order to the 1st order and the 1st order to the 0th order are 1.2123 (19.15%/15.8%) and 1.0454 (15.8%/15.11%), respectively for TE polarization. For TM polarization, the splitting ratio of efficiency of the 2nd order to the 1st order is 1.0246 (17.61%/17.18%). The ratio between efficiency of the 1st order and the 0th order is 1.1997 (17.18%/14.32%). In this optimization, we can set the duty cycle as 0.5 for easily fabrication. In addition, the optimized thicknesses of h_1 and h_2 are 1.506 μm and 1.508 μm, respectively for both TE and TM polarizations.

3. Theoretical Investigation

By performing numerical calculations, RCWA algorithm can merely numerically calculate diffraction efficiency of each diffracted order. It can not deeply excavate the light-matter interactions in such a two-layer polarization-independent grating. In fact, the incident polarized wave propagates into the grating region, it can be coupled into different grating modes. Each grating mode can have different effective index. The result of effective index can be determined by following equations for TE polarization [26]:

$$F\left(n_{eff}^2\right) = \cos k_1(1-f)d \cdot \cos k_2 f d - \frac{k_1^2 + k_2^2}{2k_1 k_2} \cdot \sin k_1(1-f)d \cdot \sin k_2 f d = \cos \varphi d \tag{6}$$

For TM polarization:

$$F\left(n_{eff}^2\right) = \cos k_1(1-f)d \cdot \cos k_2 f d - \frac{n_1^4 k_1^2 + k_2^2}{2n_1^2 k_1 k_2} \cdot \sin k_1(1-f)d \cdot \sin k_2 f d = \cos \varphi d \tag{7}$$

Where

$$k_i = k_0\sqrt{n_i^2 - n_{eff}^2},\ \varphi = k_0 \sin\theta,\ k_0 = 2\pi/\lambda \tag{8}$$

In these formulas, q is incident angle, n_i equals to 1.0 or 1.45. In our design, we set the duty cycle of 0.5 and period of 3000 nm. By substituting the given numerical parameters into above equations, we can obtain five effective indices for each polarization, where the incident wave can be coupled into five different grating modes in every grating layer. Because of the grating ridges comprise of two different materials, the distribution of modal profiles are different in two different grating layers. In fact, the ability of energy exchange between incident light and grating modes can be determined by the following overlap integrals for TE polarization [30]:

$$\left\langle E_y^{in}(x) \leftrightarrow u_q(x) \right\rangle = \frac{\left| \int_0^{d_{TE}} E_y^{in}(x) u_q(x) dx \right|^2}{\int_0^{d_{TE}} \left| E_y^{in}(x) \right|^2 \int_0^{d_{TE}} \left| u_q(x) \right|^2 dx} \tag{9}$$

For TM polarization:

$$\left\langle H_y^{in}(x) \leftrightarrow u_n(x) \right\rangle = \frac{\left| \int_0^{d_{TM}} H_y^{in}(x) u_n(x) dx \right|^2}{\int_0^{d_{TM}} \left| H_y^{in}(x) \right|^2 \int_0^{d_{TM}} \left| u_n(x) \right|^2 dx} \tag{10}$$

where the u_{q}(x) is electric field of proposed qth grating mode, the u_{n}(x) is magnetic field of the nth mode. E_{yin}(x) and H_{yin}(x) present the energies of incident polarized light. By solving above integrals and overlap integers, we obtain the values of effective index and results of energy exchange between incident light and grating modes. The values of effective index and results of energy exchange can be prohibited in Table 1.

Fig. 3 shows the distributions of modal profile in two grating layers for TE and TM polarizations with the given usual duty cycle of 0.5 and period of 3000 nm. As can be seen from Fig. 3, we can

TABLE 1
The Calculated Energy Exchange Between Incident Light and Grating Modes and Effective Indices With the Given Duty Cycle of 0.5 and Period of 3000 nm for TE Polarization and TM Polarization

Mode	0	1	2	3	4	5
TE: Layer 1, n_{eff}	1.4318	1.3761	1.2805	1.1416	0.9946	0.9160
TE: Layer 2, n_{eff}	1.9852	1.9403	1.8634	1.7511	1.5978	1.3938
TE: Overlap integers	0.4938	0	0.0885	0	0.3549	0.0484
TM: Layer 1, n_{eff}	1.4288	1.3642	1.2544	1.1053	0.9968	0.8952
TM: Layer 2, n_{eff}	1.9830	1.9312	1.8422	1.7111	1.5306	1.2928
TM: Overlap integers	0.4553	0	0.0828	0	0.3421	0.0090

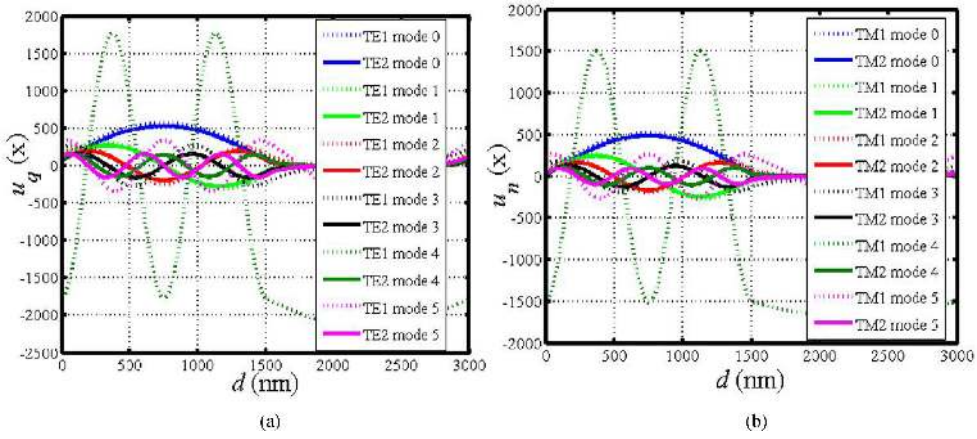

Fig. 3. The distribution of modal profile based on SMM with usual duty cycle of 0.5 and period of 3000 nm for (a) TE polarization and (b) TM polarization.

obtain the modes 0, 2, 4 are odd symmetric grating modes, modes 1, 3, 5 are even symmetric grating modes.

Fig. 4 shows the near-field distribution of electric-field and magnetic-field amplitudes for the two-layer five-port beam splitter polarization-independent grating with the period of 3000 nm and duty cycle of 0.5 for TE and TM polarizations by using a finite-difference time-domain (FDTD) method. As can be seen from Fig. 4, the energy of electric field or magnetic field in grating area can be equally distributed.

4. Study of Fabrication Tolerance and Incident Spectral Bandwidth

In practical fabrication of such a polarization-independent five-port beam splitter grating, the fabrication error is inevitable. Therefore, it is imperatively for researchers to consider the fabrication tolerance. In this design, we theoretically calculate the fabrication tolerance of our proposed optical device as shown in Fig. 5. As can be seen from Fig. 5, for keeping the good uniformity, with the scope of duty cycle varying from 0.479 to 0.487 or from 0.498 to 0.506, we can obtain the splitting ratios between diffraction orders are not more than 1.3 and the total transmission efficiency can be more than 80% for each polarization with the optimized period of 3000 nm and incident wavelength of 800 nm under normal incidence. Thus, with such moderate fabrication tolerance, it can help to fabricate five-port polarization-independent five-port beam splitter grating more conveniently.

With the development of the rapid optical communication, the broadband transmission is a basic technique. Developing more broadband gratings are necessary to meet the requirement of further optical communication. Fig. 6 displays the incident wavelength corresponding to the diffraction

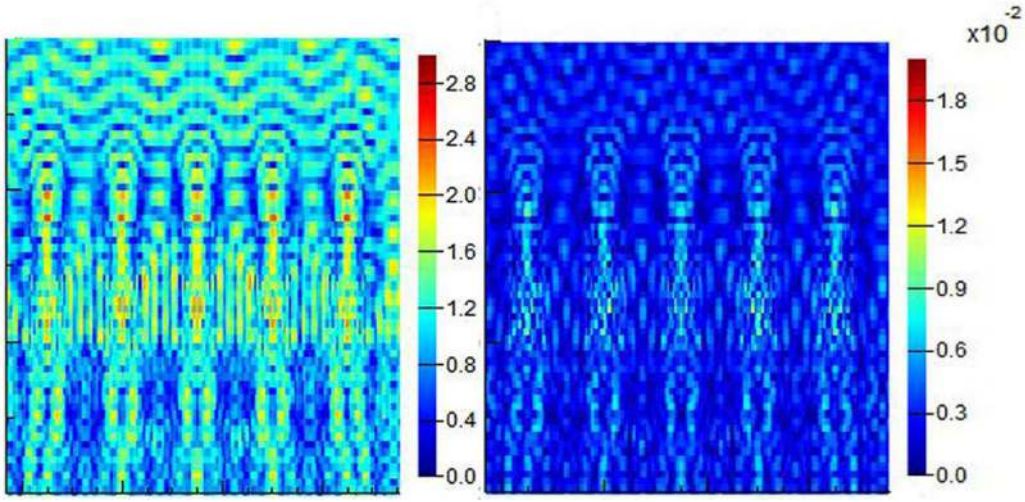

Fig. 4. The near-field distribution of (a) electric-field amplitude and (b) magnetic-field amplitude for the two-layer five-port beam splitter polarization-independent grating with the period of 3000 nm and duty cycle of 0.5 under TE or TM-polarized wave incidence.

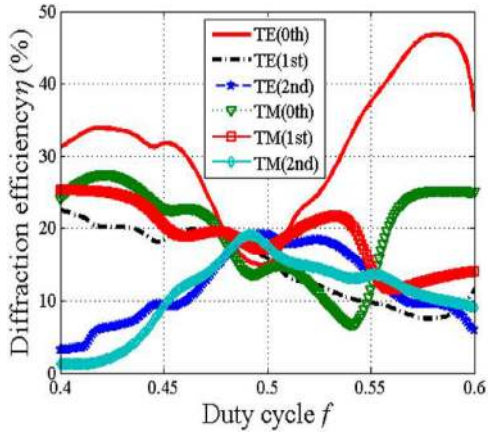

Fig. 5. The grating duty cycle versus the diffraction efficiency with the optimized grating period of 3000 nm and incident wavelength of 800 nm for TE and TM polarizations.

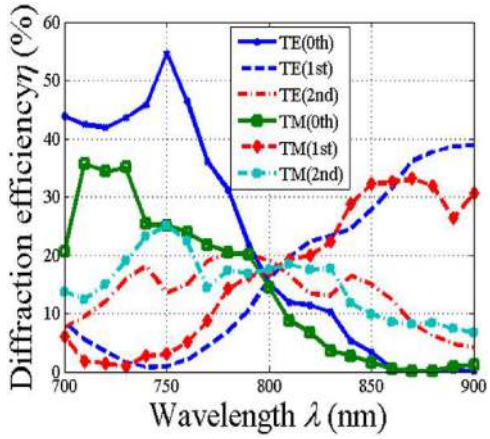

Fig. 6. Incident wavelength versus the diffraction efficiency with the optimized grating period of 3000 nm and duty cycle of 0.5 for TE and TM polarizations.

TABLE 2
Performances Comparison of Our Work to Other Conventionally Designed Reported Performances of the Five-Port Grating for TE and TM Polarizations

	Efficiency	Spectral bandwidth	Polarization property
Reported work			
TE:	η_2:19.74%,η_1:19.34%,η_0:19.46%	1515-1563 nm	Polarization dependence
TM:	η_2:19.24%,η_1:19.23%,η_0:19.49%	1541-1560 nm	
Our work			
TE:	η_2:19.15%,η_1:15.8%,η_0:15.11%	794-804 nm	Polarization independence
TM:	η_2:17.61%,η_1:17.18%,η_0:14.32%	777-801 nm	

efficiency of each diffraction order with our optimized grating period of 3000 nm and duty cycle of 0.5. As can be seen from Fig. 6, we obtain the spectral bandwidth range from 794 nm to 804 nm with the efficiency of each order more than 13% for TE polarization. For TM polarization, within the wavelength range of 777–801 nm, efficiency in each order more than 13% can be obtained. For such polarization-independent grating, we can obtain a wide spectral window of 794–801 nm.

5. Conclusion

Table 2 shows the performances comparison of our work to other conventionally designed reported performances of the five-port grating. As can be seen from Table 2, although the reported polarization-dependent five-port grating [28] can have higher diffraction efficiencies in each order for TE or TM polarization and wider spectral bandwidth when comparing to our grating, the complicated and time-consuming fabrication processes of the grating impedes such device applying in actual optical applications.

In this work, we firstly propose and design a novel two-layer five-port polarization-independent grating. However, our proposed grating can diffract into some diffraction orders with not very high efficiencies. Therefore, in the future, we should discuss potential ways for improving grating efficiency with following strategies: the first potential way is that we could design an encapsulated five-port polarization-independent grating, because such grating structure can reduce the Fresnel reflection and improve the transmission efficiencies for both TE and TM polarizations [31]. The second potential way is that we could design a triangular-groove five-port polarization-independent grating, because such special triangular-groove five-port transmission grating configuration can effectively decrease interfacial reflection on surface of the grating [32].

This paper presents a novel two-layer five-port beam splitter grating by a polarization-independent design. We firstly optimize the accurate grating parameters using RCWA algorithm. The inherent coupling mechanism happened in the grating area can be well interpreted by SMM. The near-field distribution of amplitudes for TE and TM polarizations for the five-port beam splitter grating can be simulated with the period of 3000 nm and duty cycle of 0.5 by using FDTD method. More importantly, compared with conventional reported five-port single-groove beam splitter grating under normal incidence, our proposed grating can firstly realize a polarization-independent property. In addition, the moderate fabrication tolerance and incident spectral bandwidth can be

shown. Therefore, this work can open up a possible thought for designing polarization-independent multi-port beam splitter diffraction gratings.

References

[1] O. M. Kharraz, A. S. M. Supa'at, A. F. Abas, M. T. Alresheedi, and M. A. Mahdi, "Acceleration of carrier lifetime in gain-clamped semiconductor optical amplifiers," *IEEE Photon. J.*, vol. 10, no. 5, Oct. 2018, Art. no. 7104613.

[2] D. Wang, Q. Wang, and Z. Zhang, "Polarization-independent filter based on 2-D crossed grating under oblique incidence," *IEEE Photon. J.*, vol. 10, no. 5, Oct. 2018, Art. no. 4501609.

[3] Z. Zhang *et al.*, "Low polarization-dependent-loss double-layer grating coupler for three-dimensional photonic integration," *Opt. Commun.* vol. 445, pp. 247–254, 2019.

[4] X. Duan, M. Zhang, Y. Huang, K. Liu, Y. Shang, and X. Ren, "Polarization-independent focusing reflectors using two-dimensional SWG," *IEEE Photon. Technol. Lett.*, vol. 29, no. 2, pp. 209–212, Jan. 2017.

[5] M. Hu *et al.*, "Widely tunable repetition-rate and pulse-duration nanosecond pulses from two spectral beam combined fiber amplifiers," *J. Opt.*, vol. 18, 2016, Art. no. 105501.

[6] H. Cao, C. Zhou, J. Feng, P. Lu, and J. Ma, "Design and fabrication of a polarization-independent wideband transmission fused-silica grating," *Appl. Opt.*, vol. 49, pp. 4108–4112, 2010.

[7] X. Jing, J. Zhang, S. Jin, P. Liang, and Y. Tian, "Design of highly efficient transmission gratings with deep etched triangular grooves," *Appl. Opt.*, vol. 51, pp. 7920–7933, 2012.

[8] H. Cao, C. Zhou, J. Ma, J. Wu, and S. Li, "High-efficiency fused-silica reflection grism," *Appl. Opt.*, vol. 53, pp. 2802–2805, 2014.

[9] L. Chen, X. Jing, Y. Tian, S. Jin, K. Yang, and L. Wang, "Design of a broadband high-efficiency two-port beam subwavelength grating splitter by modal method," *J. Laser Appl.*, vol. 27, 2015, Art. no. 022001.

[10] B. Wang, L. Chen, L. Lei, and J. Zhou, "Two-layer dielectric grating as two-port beam splitter," *IEEE Photon. Technol. Lett.*, vol. 25, no. 9, pp. 863–866, May 2013.

[11] J. Yang and Z. Zhou, "Double-structure, bidirectional and polarization-independent subwavelength grating beam splitter," *Opt. Commun.*, vol. 285, pp. 1494–1500, 2012.

[12] J. Feng, C. Zhou, J. Zheng, H. Cao, and P. Lv, "Dual-function beam splitter of a subwavelength fused-silica grating," *Appl. Opt.*, vol. 48, pp. 2697–2701, 2009.

[13] B. Wang, L. Chen, L. Lei, and J. Zhou, "Two-layer dielectric grating for polarization-selective beam splitter with improved efficiency and bandwidth," *Opt. Commun.*, vol. 294, pp. 329–332, 2013.

[14] G. G. Kang, Q. F. Tan, and G. F. Jin, "Polarization-selective subwavelength grating used with 193 nm light," *Opt. Commun.*, vol. 283, 4531–4535, 2010.

[15] H. Li and B. Wang, "Two-port connecting-layer-based sandwiched grating by a polarization-independent design," *Sci. Rep.*, vol. 7, 2017, Art. no. 1309.

[16] G. Zheng, J. Cong, L. Xu, and W. Su, "Compact polarizers with single layer high-index contrast gratings," *Infrared Phys. Technol.*, vol. 67, pp. 408–412, 2014.

[17] C. You *et al.*, "Optimization design and analysis of reflecting polarizing beam splitter based on metal–multilayer dielectric grating for 800 nm," *J. Mod. Opt.*, vol. 60, pp. 1598–1602, 2013.

[18] H. Guan *et al.*, "Optimization design of polarizing beam splitter based on metal-multilayer dielectric reflecting grating," *Opt. Commun.*, vol. 287, pp. 25–30, 2013.

[19] Q. Bi, J. Zheng, M. Sun, F. Zhang, X. Xie, and Z. Lin, "Design of rectangular-groove fused-silica gratings as polarizing beam splitters," *Opt. Exp.*, vol. 18, pp. 11969–11978, 2010.

[20] J. Zheng, C. Zhou, B. Wang, and J. Feng, "Beam splitting of low-contrast binary gratings under second bragg angle incidence," *J. Opt. Soc. Am. A*, vol. 25, pp. 1075–1083, 2008.

[21] Z. Sun, C. Zhou, H. Cao, and J. Wu, "Unified beam splitter of fused silica grating under the second bragg incidence," *J. Opt. Soc. Am. A*, vol. 32, pp. 1952–1957, 2015.

[22] J. Feng *et al.*, "Three-port beam splitter of a binary fused-silica grating," *Appl. Opt.*, vol. 47, pp. 6638–6643, 2008.

[23] B. Wang, "Cancellation of the zeroth order by a low-contrast grating," *Sci. Rep.*, vol. 5, 2015, Art. no. 16501.

[24] E. Gamet, A. V. Tishchenko, and O. Parriaux, "Cancellation of the zeroth order in a phase mask by mode interplay in a high index contrast binary grating," *Appl. Opt.*, vol. 46, pp. 6719–6726, 2007.

[25] M. G. Moharam, E. B. Grann, D. A. Pommet, and T. K. Gaylord, "Formulation for stable and efficient implementation of the rigorous coupled-wave analysis of binary gratings," *J. Opt. Soc. Am. A*, vol. 12, pp. 1068–1076, 1995.

[26] I. C. Botten, M. S. Craig, R. C. McPhedran, J. L. Adams, and J. Andrewartha, "The dielectric lamellar diffraction grating," *Opt. Acta*, vol. 28, pp. 413–428, 1981.

[27] H. Li, B. Wang, H. Pei, L. Chen, L. Lei, and J. Zhou, "Fused-silica sandwiched three-port grating under second Bragg angle incidence," *Superlatt. Microstruct.*, vol. 93, pp. 157–162, 2016.

[28] C. Gao *et al.*, "Coupling mechanism and field distribution of reflective grating for 1×5 splitting," *Opt. Commun.*, vol. 452, pp. 395–399, 2019.

[29] C. Xiang, C. Zhou, W. Jia, and J. Wu, "Five-port beam splitter of a single-groove grating," *Chin. Opt. Lett.*, vol. 16, 2018, Art. no. 070501.

[30] T. Clausnitzer *et al.*, "An intelligible explanation of highly-efficient diffraction in deep dielectric rectangular transmission gratings," *Opt. Exp.*, vol. 13, pp. 10448–10456, 2005.

[31] T. Clausnitzer, T. Kämpfe, F. Brückner, R. Heinze, E.-B. Kley, and A. Tünnermann, "Reflection-reduced encapsulated transmission grating," *Opt. Lett.*, vol. 33, pp. 1972–1974, 2008.

[32] L. Chen, X. Jing, L. Wang, J. Zhang, S. Jin, and Y. Tian, "Broadband antireflection enhancement by triangular grating microstructure in the resonance domain," *Opt. Laser Technol.*, vol. 62, pp. 95–108, 2014.